Available online at www.sciencedirect.com
ScienceDirect
Journal of Power Sources 175 (2008) 408–418
JOURNAL OF POWER SOURCES
www.elsevier.com/locate/jpowsour

Water flux in membrane fuel cell humidifiers: Flow rate and channel location effects

P. Cave [a], W. Mérida [a,b,*]

[a] *Clean Energy Research Centre, University of British Columbia, Vancouver, BC, Canada V6T 1Z4*
[b] *Institute for Fuel Cell Innovation, 4250 Wesbrook Mall, Vancouver, BC, Canada V6T 1W5*

Received 19 July 2007; accepted 31 August 2007
Available online 7 September 2007

Abstract

A straight, single channel membrane humidifier was constructed to measure temperature and moisture profiles along both the donor and receiver channels. A persulfonic Nafion membrane was used as the water exchange medium.

We report on results obtained with single-phase vapour-to-vapour, counter flow operation. First, the heat loss to the surroundings was quantified and found to affect the overall performance significantly. Second, the results from varying flow rates indicate that lower flow rates lead to higher outlet dew point values of the receiver stream which can be related to longer residence times. It was also found that moisture transfer is more strongly influenced by the flow rate through the receiver side than the donor side. Finally, five-point dew point profiles for both donor and receiver sides are reported for various temperature conditions. No stream wise variation in moisture flux was observed, and the average flux value increased from 3.3×10^{-5} kg s^{-1} m^{-2} at 30 °C to 2.0×10^{-4} kg s^{-1} m^{-2} at 70 °C under fully humidified donor-side inlet conditions.

Keywords: Humidifier; Membrane; Fuel cell; Water management; Mass transfer; Single phase

1. Introduction

One of the largest obstacles in the way of proton exchange membrane fuel cells (PEMFC) achieving commercial viability is the cost and size of the system. At least two ways to reduce cost and size are increasing power density (via water management, catalysts, materials, etc.) and trimming balance of plant costs. Reactant humidification subsystems are among the most expensive components in the balance of plant, and in addition can be a key performance enhancer. Technological improvements to reactant humidification will have a beneficial impact on the system power density and cost.

Traditional stack humidification techniques such as saturation bubblers, direct injection, spray injection, etc., are being replaced by smaller, simpler, and more cost-effective solutions. Current stack humidification strategies are enthalpy wheels, self-humidification, and membrane humidifiers. Enthalpy wheels use a motor to rotate a desiccant-coated porous cylindrical core between the wet stream and dry stream. The core absorbs heat and moisture while exposed to the wet stream, and then cools and desorbs the moisture once rotated to the dry stream. This unit is advantageous because it is compact, effective, and has a very low pressure drop, but it is disadvantageous because it has numerous moving parts and seals, is expensive and demands an extra parasitic load to operate the rotary motor.

Self-humidification methods [1,2] attempt to deliver water to the membrane using water or water-producing mechanisms available internally. Watanabe and co-workers have reported on self-humidified PEMFCs using a very thin membranes impregnated with particles of SiO_2, TiO_2, and Pt [1]. The oxides are highly hygroscopic and increase water retention. The noble catalyst enhances water production from $H_{2(g)}$ and $O_{2(g)}$ that diffuse through the thin membrane and react internally. These authors maintain that the parasitic fuel losses are justified by the improved performance of the ionic conductor. However, the effects on membrane longevity and the membrane electrode

Abbreviations: DPAT, dew point approach temperature (°C) or (K); EE, enthalpy exchange effectiveness; LE, latent heat transfer effectiveness; SE, sensible heat transfer effectiveness; WRR, water recovery ratio.

* Corresponding author. Permanent address: Clean Energy Research Centre, University of British Columbia, 6250 Applied Science Lane, Vancouver, BC, Canada V6T 1Z4. Tel.: +1 604 822 4189; fax: +1 604 822 2403.
E-mail address: walter.merida@ubc.ca (W. Mérida).

0378-7753/$ – see front matter © 2007 Elsevier B.V. All rights reserved.
doi:10.1016/j.jpowsour.2007.08.103

Nomenclature

A	membrane surface area (m^2)
c_p	specific heat at constant pressure ($J\,mol^{-1}\,K^{-1}$)
h	enthalpy ($J\,kg^{-1}$)
$\bar{J}_{mem,H_2O}$	average water flux across membrane ($kg\,s^{-1}\,m^{-2}$)
L	length of channel, 0.2 m (m)
$\dot{m}$	mass flow rate ($kg\,s^{-1}$)
MW	molecular weight ($kg\,mol^{-1}$)
$p^{sat}_{H_2O}$	saturation vapour pressure (Pa)
p	total pressure (101,325 Pa unless specified otherwise) (Pa)
p_{H_2O}	water vapour partial pressure (Pa)
Q	volumetric flow rate (SLPM)
q'	heat transfer rate to surroundings per unit length ($W\,m^{-1}$)
R^2	coefficient of determination
T	temperature (K or °C)
T_d	dew point above liquid water (K)
t_{mem}	membrane thickness (m)
U	overall heat transfer coefficient ($W\,m^{-2}\,K^{-1}$)
w	effective perimeter for heat transfer to surroundings (m)
x	distance along channel measured from dry-side inlet (wet-side inlet is at $x = L$) (m)

Greek letters

ε	effectiveness [0,1]
γ_{mem}	membrane conductivity ($W\,m^{-1}\,K^{-1}$)
λ	stoichiometric ratio
ξ	relative humidity [0,1]
ω	humidity ratio, or specific humidity ($kg_{H_2O}\,kg^{-1}_{dry\ air}$)

Subscripts

H_2O	water vapour
air	air
WI	wet-side channel inlet (also used as an abbreviation)
WO	wet-side channel outlet (also used as an abbreviation)
DI	dry-side channel inlet (also used as an abbreviation)
DO	dry-side channel outlet (also used as an abbreviation)
surr	surroundings
wet	wet-side channel
dry	Dry-side channel
x	all probe locations along channel

assembly response to sudden changes in current density are not clear.

Although several conditioning schemes have been proposed to run PEMFC stacks on dry reactants, these schemes are only effective for low power applications (<5 kW) working at low temperatures (<60 °C) [3]. Larger power applications require direct reactant humidification almost without exception. The reasons behind this requirement are not restricted to operational constraints, and they can be explained by the fundamental properties of humidified gas mixtures. Larminie and Dicks considered a PEMFC operating on dry reactants [3]. They treated the water vapour and the exiting streams as perfect gases, and assumed that all the product water was evaporated. With these assumptions, they calculated the partial pressure of water in terms of the total pressure at the cathode outlets, and the flow stoichiometry of dry air. Mérida reviewed these calculations [4] and used the resulting expressions to generate the curves in Fig. 1. These calculations illustrate that the stringent water requirements within a PEMFC restrict operation to a very narrow range (i.e., a range for which $\xi = 1 \pm \delta\xi$, where $\delta\xi$ is small). Operating temperatures higher than 60 °C (which are desirable to minimise activation losses) correspond to very drying conditions for all practical flows at low pressures.

A third type of humidification subsystem is a membrane humidifier. These passive devices recover humidity from the cathode exhaust and transfer it through a hygroscopic membrane to the cathode inlet stream (dry air). Two architectures are currently in use, both derived from compact heat exchanger designs. In the shell and tube design, the dry stream flows inside a bank of small membrane tubes while the wet stream flows over and around the bank of tubes. The plate and frame architecture consists of membranes stacked on top of each other with a flow field plate separating the layers to allow flow. Membrane humidifiers are capable of a high moisture transfer capability at a reasonable pressure drop. This work characterizes a single channel version of a membrane humidifier.

While humidifiers can be constructed with other membranes, Nafion membranes are the standard heat and mass transfer medium in a commercial membrane humidifier. The under-

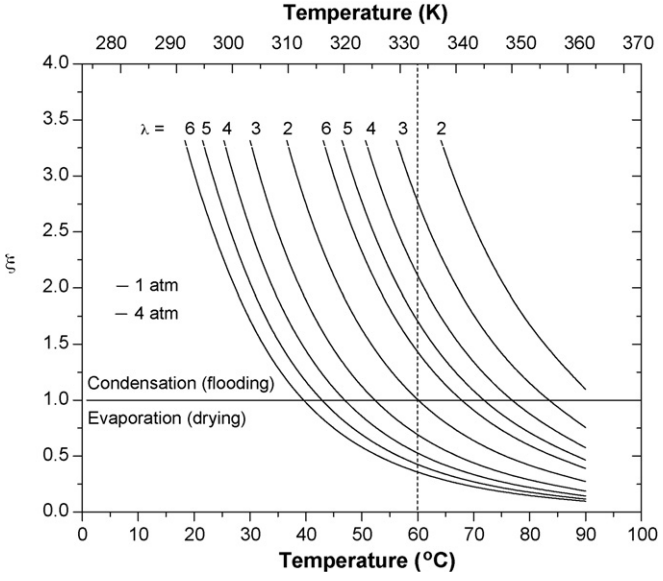

Fig. 1. The variation of relative humidity at the cathode outlets as a function of temperature, stoichiometry, and operating pressure [4], adapted from [3].

standing of water transport through Nafion has been the focus of intense analytical and experimental efforts. The work by Springer et al. in 1991 [5] was the first of many papers to model the diffusion of water as a phenomenon driven by a chemical activity (water content) gradient. The water content of the membrane is calculated as a function of relative humidity from equilibrium sorption curves [6,7]. In practical fuel cell operation, however, the membrane usually does not achieve sorption equilibrium, which can take between 100s and 1000s [8]. Only a few models consider the significance of surface mass transfer effects [8–11]. These models use a mass transfer conductance to relate the bulk gas water concentration to the water content on the membrane surface. The work of Ge et al. [8] goes a step further and suggests the absorption and desorption coefficients have a linear dependence on water content.

The specific application of cathode humidifiers has not been given much attention in the literature until recently. In a notable early work Nguyen and White [12] discussed the effects of different humidification strategies on PEMFC performance. However, most of these techniques are outdated now. More recently, Chen and Peng [10] reported on a transient model of a planar humidifier in Simulink in the context of control systems. Other relevant literature can be found in the field of energy recovery devices used to recuperate heat and humidity in building ventilation systems [13–15]. Zhang and collaborators have extended heat transfer NTU analysis to mass transfer across membranes [14].

Experimental efforts to examine PEMFC membrane humidifiers have been sparse. Most experimental efforts involve condensing the outlet stream to obtain a time and space-averaged flux value for moisture transport across the membrane [16]. These flux values have been tabulated against geometric parameters such as the ratio of residence time (e.g., the residence time that water molecules spend in the flow channel) to diffusion time (e.g., the time required to diffuse through air over the depth of the channel) [16,17]. This ratio has been used successfully to specify the optimal operating ranges for planar humidifiers and to convert the windows in parameter space into design specifications. Other experimental work was provided by Park et al. in 2005 [18], who reported data for liquid water-to-gas internal humidification using multiple membranes.

In this work, we report the effects of flow rates on performance of planar membrane humidifiers operating under single phase conditions. We then address a gap between simulations based on analytical models and the macroscopic experimental studies. The former provide complete spatial mapping of humidity and temperature while the latter rely on time and space-averaged fluxes. We provide humidity measurements at different locations along the channels to assist ongoing modeling efforts.

2. Experimental

2.1. Setup

The experimental setup consisted of a single channel membrane humidifier as illustrated in Fig. 2. A 1 cm × 1 cm × 20 cm flow channel was machined into two plates, which were then mated together with Nafion 117 membrane as the hygroscopic separator. The Nafion was pretreated by boiling in a 3 wt.% H_2O_2 solution for 2 h, rinsing with de-ionized water, boiling in 1.0 M H_2SO_4 for 2 h, and finally rinsing and storing in de-ionized water. The membrane was removed from de-ionized water and exposed to ambient room temperature and humidity conditions for at least 24 h prior to testing. Five evenly spaced 1/16 in. probe holes were drilled into the flow channels for thermocouple or dew point sensor placement. Calibrated type-T unsheathed thermocouples were used due to their reasonable accuracy, suitability in moist air environments, and small size (to minimize interference with the flow distribution in the channel).

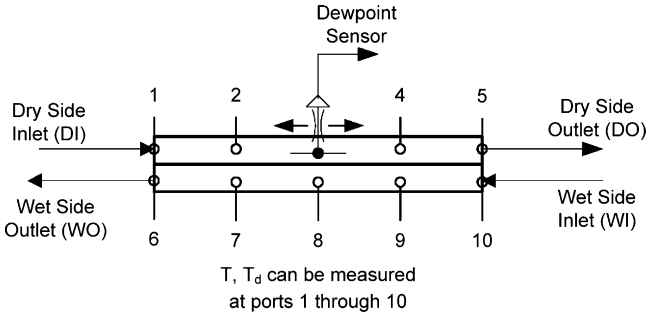

Fig. 2. Single channel humidifier.

A Vaisala HMT337 dew point transmitter was used to measure moisture content. Because this is a polymer-based capacitive sensor, an effort was made to ensure the probe temperature was equal to the process temperature. The dew point probe was placed in a cavity, and at the time of measurement a sample of gas from the channel was allowed to flow through this cavity to perform accurate dew point measurements. The Vaisala meter measures relative humidity at ±2% and temperature at ±0.2 °C. The Hyland and Wexler equation was used throughout this work to relate saturated water vapour pressure to temperature:

$$\ln p^{\mathrm{sat}}_{\mathrm{H_2O}} = \frac{C_1}{T} + C_2 + C_3 T + C_4 T^2 + C_5 T^3 + C_6 \ln(T) \quad (1)$$

where T is in Kelvin and $p^{\mathrm{sat}}_{\mathrm{H_2O}}$ is in Pa. The constant coefficients are listed in Table 1.

In this work, dew points below 0 °C refer to the temperature at which the parcel of moist air would be saturated above super cooled liquid water. This is distinct from the frost point, which correlates moisture content to the saturation pressure above a frozen surface (i.e., ice). In all cases,

Table 1
Coefficients in Hyland and Wexler saturation vapour pressure equation

C1	-0.58002206×10^4
C2	0.13914993×10^1
C3	$-0.48640239 \times 10^{-1}$
C4	$0.41764768 \times 10^{-4}$
C5	$-0.14452093 \times 10^{-7}$
C6	0.65459673×10^1

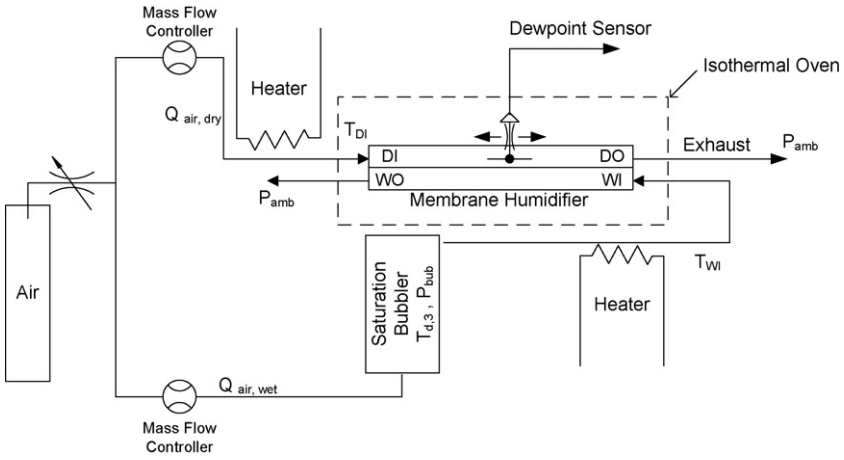

Fig. 3. Experimental setup schematic.

however, negative dew point values indicate very low water concentrations.

Fig. 3 shows the experimental setup. The dry side stream (or receiver side) was delivered through a mass flow controller and heated to the desired inlet temperature, T_{DI}. The wet side stream (or donor side) passed through a mass flow controller, a saturation point bubbler humidifier, and then heated to the desired temperature, T_{WI}. The moisture content of this stream was controlled by the temperature and pressure in the bubbler. In actual operation, the wet side stream, coming from the cathode exhaust, would be oxygen-depleted moist air. In this work, regular air was used on both sides.

2.2. Methodology

Three related questions were addressed in this work. First, in our configuration, the heat lost to the surroundings was comparable to the enthalpic flow through the humidifier and thus not negligible. The first step then was to characterize and quantify the heat loss of the humidifier. A stream may gain or lose heat energy through the channel walls to the surroundings, through the membrane to the opposite stream, and through latent heat transfers in the presence of phase changes. Single phase conditions were imposed throughout this work for simplicity, although in practical operating conditions there may be condensation on the wet side.

Next, the effects of flow rates were studied. The effect of flow rates on humidifier performance is of utmost interest in humidifier design because it characterizes the humidifier just as a polarization curve characterizes a fuel cell. The fuel cell system's air flow rate will be determined by the stoichiometric ratio and current demands, so it is desirable to characterize the humidifier's moisture-transferring ability as a function of flow rate. Furthermore, membrane humidifiers are currently passive devices, humidifying the reactant as much as possible before entering the cell. However, in some operating regimes or future applications, it may be desirable to control the humidity over a range. One example of a control mechanism is a dry air bypass gate as suggested in [10]. In this case, there would be a differential flow on either side of the membrane. It would then be advantageous to fully understand the tradeoffs of changing wet side and dry side flow rates individually.

A randomized full-factorial experiment was carried out with three replications at three levels of both wet side and dry side flow rates under four sets of conditions. The experimental conditions for each case are summarized in Table 2.

The third portion of this study aimed to provide information regarding the stream-wise variation in moisture flux. Knowing where most of the moisture transfer occurs in counter flow mode could provide valuable information leading to optimization of the channel length. Two replications with randomization were taken at each of the 10 probe locations. This was performed for the same four sets of conditions.

The seven independent variables that can be varied in this arrangement are: dry inlet temperature, dew point, and flow rate (T_{DI}, $T_{d,DI}$, and $Q_{air,DI}$), wet side inlet temperature, dew point, and flow rate (T_{WI}, $T_{d,WI}$, and $Q_{air,WI}$) and the temperature of the surroundings (T_{surr}). The dependent variables can include temperatures or dew points at the 10 probe locations, T_x or $T_{d,x}$. Due to the high number of variables, four individual cases representing different operating regimes were considered. The case definitions and experimental testing approach is shown in Table 2: Testing Matrix.

2.3. Measurement technique

Fig. 4 illustrates the dew point measurement technique. In steady state, if the convective velocity of the air/water mixture along the channel is greater than the diffusive velocity of water in air across the channel, then a significant concentration gradient in the y-direction will develop. As a result, the sample probe location on the wall opposite the membrane may measure an artificially low concentration value on the dry side and an artificially high concentration value on the wet side. This effect will become more noticeable further along the channel were concentration gradients grow larger and the mixture is no longer well-mixed. To mitigate this effect, the channel exit stream was partially restricted during measurements to force a larger sample of air/water mixture through the sensing cavity.

Table 2
Testing matrix

Case	Research focus	Fixed temperatures in (°C) flows in (SLPM)	Independent	Dependent
Case 1: non-isothermal case	Heat loss to surroundings	$T_{DI} = 85$ $T_{d,DI} = -40$ $Q_{air,\,DI} = 1.0$ $T_{WI} = 85$ $T_{d,WI} = 25$[a] $Q_{air,WI} = 1.0$ $T_{surr} = 21$	Streamwise location	T_x
	Effect of flow rates on moisture transfer	$T_{DI} = 25$ $T_{d,DI} = -40$ $T_{WI} = 80$ $T_{d,WI} = 25$[a] $T_{surr} = 21$	$0.4 < Q_{air,DI} < 1.0$ $0.4 < Q_{air,WI} < 1.0$	$T_{d,DO}$
	Streamwise variation in moisture flux	As above, with $Q_{air,DI} = 1.0$ $Q_{air,WI} = 1.0$	Streamwise location	$T_x, T_{d,x}$
Cases 2, 3, and 4[b]: isothermal cases at low, medium, and high temperatures, respectively	Effect of flow rates on moisture transfer under isothermal conditions	$T_{DI} = T_{surr}$	$0.4 < Q_{air,\,DI} < 1.0$	$T_{d,DO}$
		$T_{d,DI} = -40$ $T_{WI} = T_{surr}$ $T_{d,WI} = T_{surr}$ Where $T_{surr} = 30$ (Case 2) $T_{surr} = 50$ (Case 3) $T_{surr} = 70$ (Case 4)	$0.4 < Q_{air,\,WI} < 1.0$	
	Streamwise variation in moisture flux	As above, with $Q_{air,DI} = 1.0$ $Q_{air,WI} = 1.0$	Streamwise location	$T_{d,\,x}$

[a] This is the maximum dew point allowable to ensure no condensation occurs in the wet side as the temperature drops; limited by humidifier heat loss to the surroundings.
[b] These cases use an oven to impose isothermal conditions.

3. Theory

3.1. Flow correction

As a result of the experimental set up shown in Fig. 3, one must consider the addition of water when stating the actual wet side flow rate delivered to the membrane humidifier. The amount of added water is quantified, assuming an ideal gas mixture and 100% effective bubbler, via:

$$\dot{m}_{H_2O} = \frac{p^{sat}_{H_2O}}{p - p^{sat}_{H_2O}} \frac{MW_{H_2O}}{MW_{air}} \dot{m}_{air} \quad (2)$$

where $p^{sat}_{H_2O}$ is the saturation pressure at the bubbler temperature, and p is the total pressure in the bubbler. The mass flow rate of water and air are summed to determine the actual flow composition and rate delivered to the membrane humidifier. For reference, Fig. 5 has been included to show the appropriate correction factors (either volumetric or gravimetric) to obtain the total flow rate of the mixture. Higher backpressure build up at the saturation bubbler results in less water being evaporated by the flow. Should one not account for these corrections, the maximum error will be found in cases with high dew point and high flow rates (which cause higher back pressures). The sensitivity to dew point is much higher than to bubbler pressure.

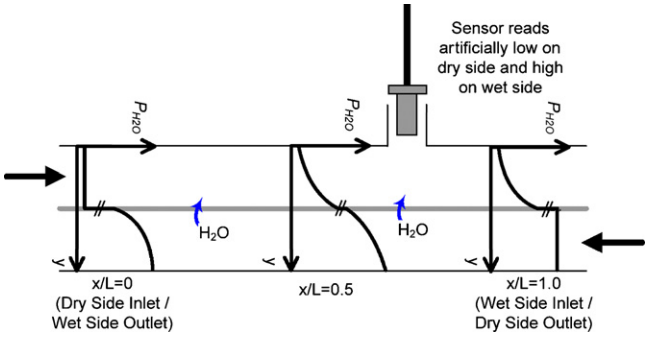

Fig. 4. The measurement technique showing conceptually the concentration gradients across the channel and their effect on measurement precision.

3.2. Performance metrics

Several candidate metrics to measure a humidifier's moisture-transferring ability have been used in the past. The stream of

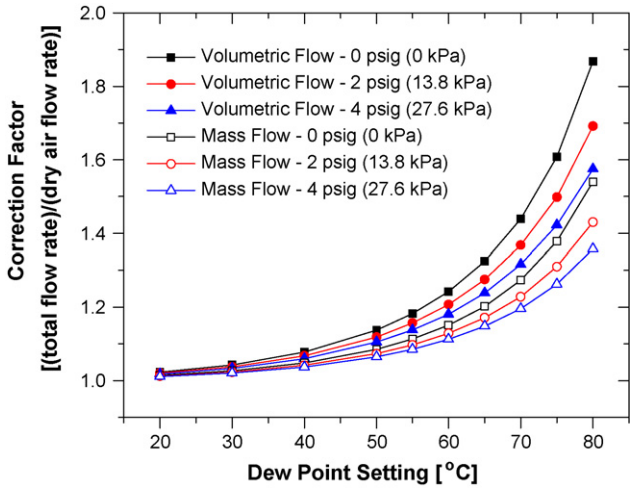

Fig. 5. Volumetric and mass flow rate correction factors due to addition of water for various bubbler backpressures.

interest is the dry side outlet which will be delivered to the cathode and the variable of interest is the amount of water carried in that stream. An appropriate performance metric often depends on whether one is comparing different humidifiers at identical conditions or comparing the same humidifier at different conditions. Generally, however, outlet relative humidity and outlet dew point are poor choices because the temperature (if using relative humidity), pressure, and flow rate are still needed to quantify the flow rate of water present in the stream. Furthermore, there is no indication of the maximum value that could have been attained under the conditions.

The dew point approach temperature (DPAT) is the difference in dew point between wet side inlet and dry side outlet—a lower DPAT is indicative of better performance. When comparing different humidifiers or the same humidifier at conditions with constant wet side inlet dew point, the DPAT provides a practical evaluation of the performance. To exemplify an area of caution when using DPAT, consider the case where a non-perfect humidifier is run with $T_{d,WI} = 40\,^{\circ}C$ and yields a DPAT of 5 °C. If it is then run under the same flows with $T_{d,WI} = 80\,^{\circ}C$ and yields a DPAT of 30 °C, the DPAT performance is worse but it has in fact transferred more water. Also, DPAT is a skewed scale due to the nature of the saturation pressure curve; a 3 °C DPAT is not twice as good as a 6 °C DPAT.

The total water transfer is calculated as the difference in amount of water between inlet and outlet on either stream. The average water flux is the total water transfer normalized by total membrane area:

$$\bar{J}_{\mathrm{mem,H_2O}} = \frac{\dot{m}_{\mathrm{H_2O,DO}} - \dot{m}_{\mathrm{H_2O,DI}}}{A} \tag{3}$$

where the mass flow rates of water, $\dot{m}_{\mathrm{H_2O,DO}}$ and $\dot{m}_{\mathrm{H_2O,DI}}$ are calculated using Eq. (2) with $p^{\mathrm{sat}}_{\mathrm{H_2O}}$ replaced with the water vapour partial pressure, $p_{\mathrm{H_2O}}$. Either the total water transfer or average water flux are suitable metrics when comparing the same humidifier at different operating conditions, but only the total water transfer is suitable when comparing different humidifiers. Note, however, that these metrics have no indication of the maximum amount that could have been transferred.

There are several first Law effectiveness measures which normalize humidifier performance on a scale from 0 to 1. The WRR is defined as the ratio of the total water transferred to the quantity of water available in the wet stream:

$$\mathrm{WRR} = \frac{\dot{m}_{\mathrm{H_2O,DO}} - \dot{m}_{\mathrm{H_2O,DI}}}{\dot{m}_{\mathrm{H_2O,WI}}} \tag{4}$$

The WRR is only suitable if running on dry reactants, otherwise the maximum amount that could be transferred is less than $\dot{m}_{\mathrm{H_2O,WI}}$. The sensible, latent (or moisture), and enthalpy (or total) effectiveness factors for heat and moisture transfer devices are defined as:

$$\varepsilon = \frac{\dot{m}_{\mathrm{air,DI}}(X_{\mathrm{DO}} - X_{\mathrm{DI}})}{(\dot{m}_{\mathrm{air}})_{\mathrm{min}}(X_{\mathrm{WI}} - X_{\mathrm{DI}})} \tag{5}$$

where X is either the temperature (T), humidity ratio (ω), or enthalpy (h) depending on whether the sensible effectiveness (SE), latent effectiveness (LE), or enthalpy effectiveness (EE) is being calculated. The SE is a measure of heat transfer; not mass transfer, and therefore is of limited use in humidifier design. The LE and EE are useful measures and correct the WRR in the case of partially humidified dry side inlet conditions. EE can be misleading from a moisture transfer point of view if the sensible heat exchange makes up the bulk of the total enthalpy exchange. The LE is the better of the three to isolate moisture-transferring effectiveness.

Finally, a deficiency of all of these effectiveness parameters is that they only consider mass and energy conservation. Second law considerations such as irreversibilities due to heat transfer, phase changes, absorption/desorption, and friction losses are not accounted for so a thermodynamic maximum performance is difficult to predict.

4. Results and discussion

4.1. Heat loss to surroundings

The amount of heat lost to the surroundings was quantified by how it affects the temperature profiles in co-flow operation with both inlet streams flowing dry air at the same temperature. Neglecting changes in potential or kinetic energy, the heat loss per unit length for this configuration, q' (W m^{-1}), was calculated according to the equation:

$$q' = -\frac{\mathrm{d}(\dot{m}c_{\mathrm{p}}T)}{\mathrm{d}x} = -\dot{m}c_p\frac{\mathrm{d}T}{\mathrm{d}x} \tag{6}$$

The derivative of the quadratic fit ($R^2 = 1.00$) shown in Fig. 6, the appropriate flow rate, and the specific heat capacity of dry air ($c_p = 1007\,\mathrm{J\,kg^{-1}\,K^{-1}}$) were used to calculate the heat loss rate. If the heat loss to the surroundings is modeled with an overall heat transfer coefficient, the following equation applies [19]:

$$q' = Uw(T_{\mathrm{surr}} - T) \tag{7}$$

And the product of overall heat transfer coefficient, U, and effective perimeter, w, can be extracted from the slope of a

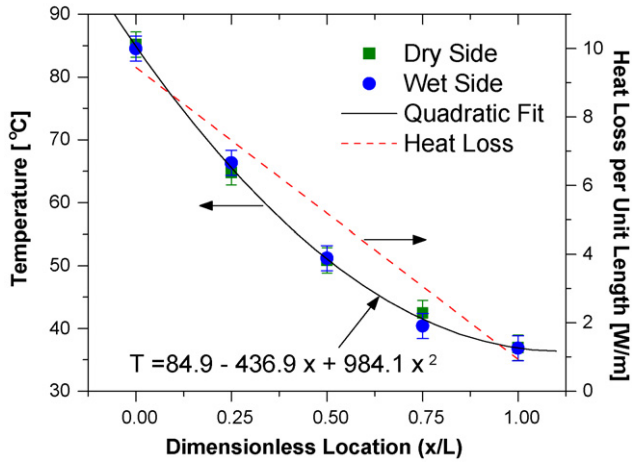

Fig. 6. The temperature profile and the heat loss rate to surroundings with dry air in coflow mode (1.0 SLPM).

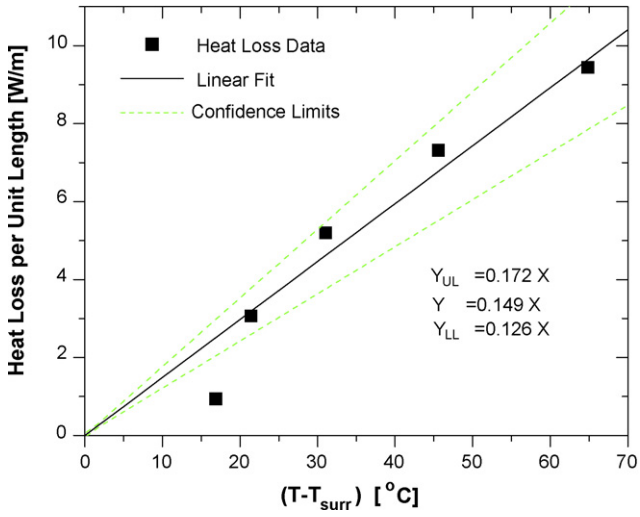

Fig. 7. Determination of overall heat transfer coefficient.

linear fit in a plot of q' versus $(T_{surr} - T)$ (Fig. 7). A value of $Uw = 0.149 \pm 0.023$ W K^{-1} m^{-1} at a 95% confidence interval was obtained for this particular experimental setup. The Uw term can be assumed constant for fully developed laminar flows because the Nusselt numbers, thermal conductivity of air, and consequently convective heat transfer coefficients all remain approximately constant.

4.2. *Effect of flow rates on humidification performance*

Reporting solely the outlet dew point or relative humidity [18] as the performance variable can be misleading because it is possible and common to find that a lower outlet dew point at a higher flow rate can represent more mass of water transferred than a higher dew point reading at a lower flow rate. Therefore, the average water flux across the membrane and WRR performance indicators are also considered in the current section. The WRR is suitable as an effectiveness measure because the dry side inlet was dry air in all cases. Contours of these three metrics for the ranges of flow studied are shown in Figs. 8–11.

Two observations can be made with regard to Figs. 8a, 9a, 10a, and 11a. First, in all cases the outlet dew point increases at lower flow rates. This result might be expected since lower flow rates give both the wet and dry gases a longer residence time in the channel, allowing for more moisture to be evaporated. Second, the effect of the dry side flow rate on outlet dew point is generally much more pronounced than the wet side flow rate (evidenced by the near-vertical contour lines). This suggests that an abundance of moisture exists at the membrane interface on the dry side and it is only the dry side's time in the channel that limits how much water is evaporated.

Figs. 8b, 9b, 10b, and 11b uncover no clear trends from case to case. However, it should be noted that a higher outlet dew point does not necessarily mean that more moisture has been transferred (in many cases the opposite is true). This is an important consideration when comparing performance data because using dew point alone may lead to erroneous interpretations. For example, Park et al. [18] concluded that flux across the membrane increases with an increase in flow rates, whereas Ge et al. [8], in a similar application, concluded that the outlet dew point decreases with increasing flow rates. The two conclusions

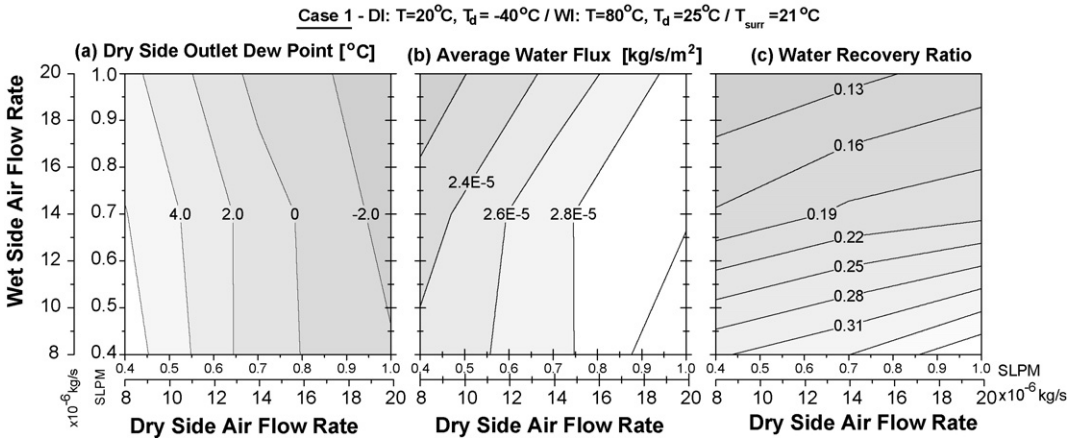

Fig. 8. Case 1 (non-isothermal)—effect of flow rates on (a) outlet dew point, (b) average water flux, and (c) water recovery ratio.

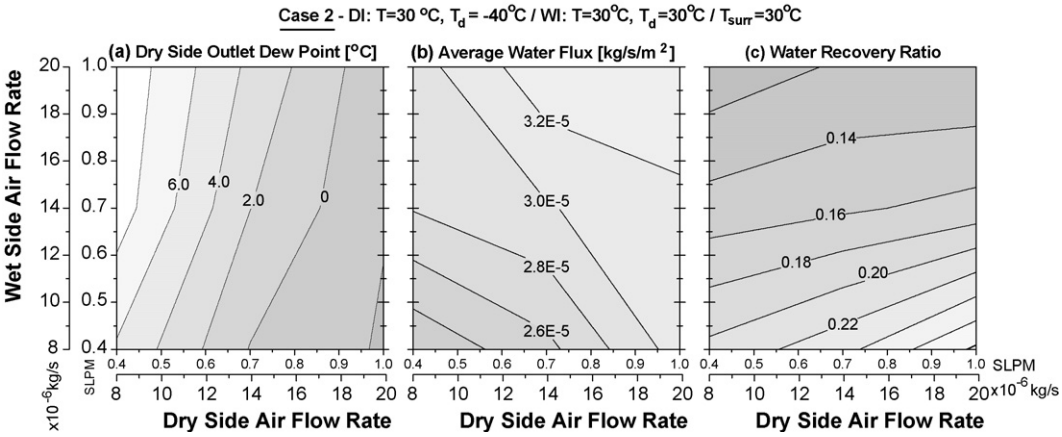

Fig. 9. Case 2 (isothermal, 30 °C)—effect of flow rates on (a) outlet dew point, (b) average water flux, and (c) water recovery ratio.

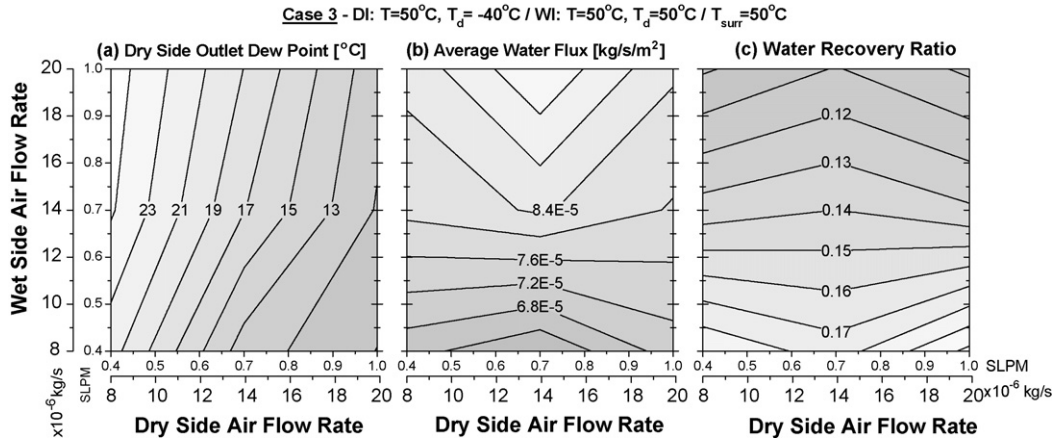

Fig. 10. Case 3 (isothermal, 50 °C)—effect of flow rates on (a) outlet dew point, (b) average water flux, and (c) water recovery ratio.

appear in conflict, but are solely the result of the metric used to indicate performance. A second observation with respect to these graphs is that there exists an optimal combination of flow rates that yields the highest water flux. However, this optimum varies with operating conditions in an unclear way and in some cases is not reliably discernible with the data presented here (Fig. 11b). Nonetheless, the importance of such information can be illustrated with an example. If operating at 50 °C (Fig. 10b) with both $Q_{air,DI}$ and $Q_{air,WI}$ at 1.0 SLPM, bypassing a portion of the dry side flow to allow only 0.7 SLPM through the dry side of the humidifier would enable more water to be transferred. The two streams could then be remixed with a higher specific humidity than if all of the dry air had been passed through the humidifier.

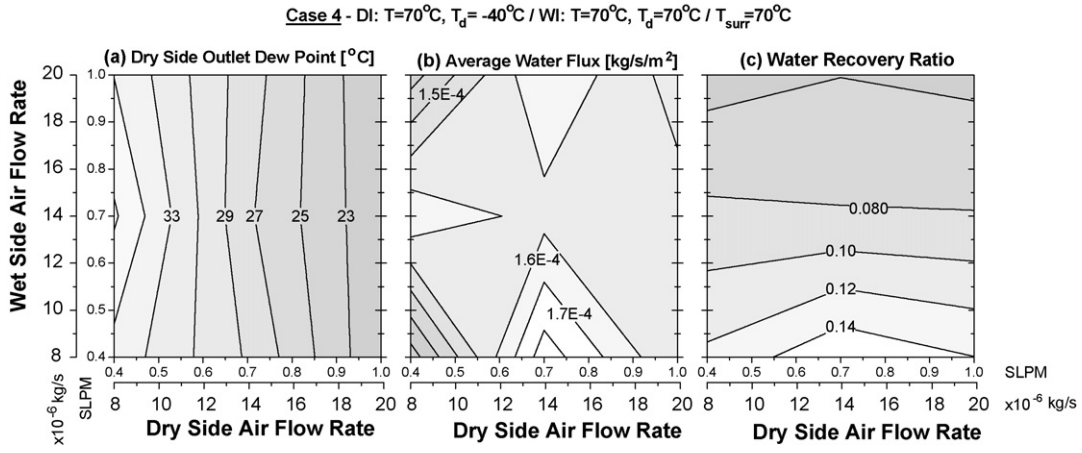

Fig. 11. Case 4 (isothermal, 70 °C)—effect of flow rates on (a) outlet dew point, (b) average water flux, and (c) water recovery ratio.

Table 3
Calculated accuracy and precision estimates for dew point readings in factorial experiments

Wet side (SLPM)	Accuracy[a] (±°C) dry side flow rate (SLPM)			Precision[b] (±°C) dry side flow rate (SLPM)		
	0.4	0.7	1.0	0.4	0.7	1.0
Case 1						
0.4	1.38	1.66	1.94	1.16	1.37	0.50
0.7	1.41	1.65	2.07	0.75	0.79	0.05
1.0	1.47	1.79	2.12	0.02	0.86	0.18
Case 2						
0.4	0.80	1.10	1.20	2.07	2.12	2.89
0.7	0.71	0.99	1.18	1.89	1.73	1.45
1.0	0.70	0.91	1.17	0.70	0.98	0.24
Case 3						
0.4	0.90	1.32	1.44	0.61	0.95	3.16
0.7	0.86	1.09	1.37	1.86	2.50	2.05
1.0	0.85	1.00	1.33	0.69	1.75	1.14
Case 4						
0.4	1.22	1.46	1.71	2.59	2.02	1.65
0.7	1.10	1.51	1.70	0.66	3.08	0.98
1.0	1.20	1.49	1.72	0.84	2.54	1.75

[a] Based on manufacturer's published accuracy limits for given conditions.
[b] Based on standard deviation of three replications.

All cases exhibit similar trends on the water recovery ratio graphs; better effectiveness at high dry side flow rates and low wet side flow rates. Note, however, that a high effectiveness rating (a relative measure) does not necessarily mean the design will meet its performance specification in absolute terms (kg s^{-1} m^{-2}). As the temperature increases from Case 2 to Case 4, the WRR values become progressively smaller. At equal flows of 0.7 SLPM, the WRR goes from 0.16 at from 30 °C to 0.082 at

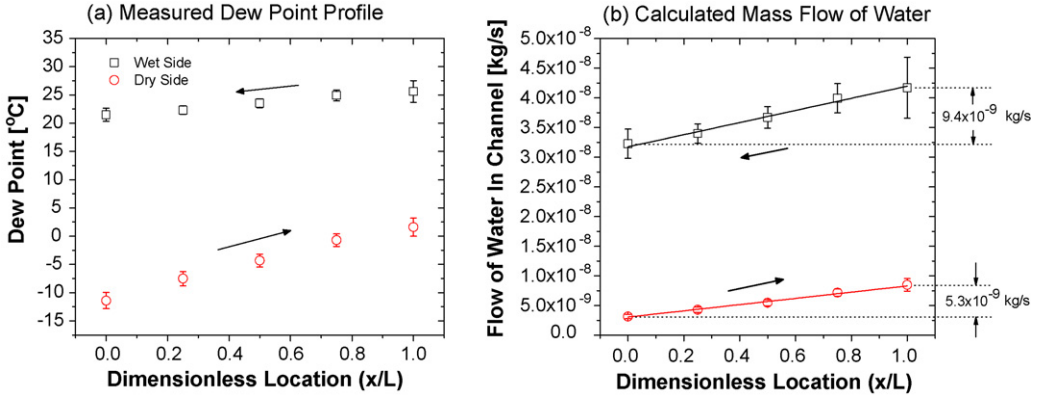

Fig. 12. Moisture profiles—Case 1 (non-isothermal).

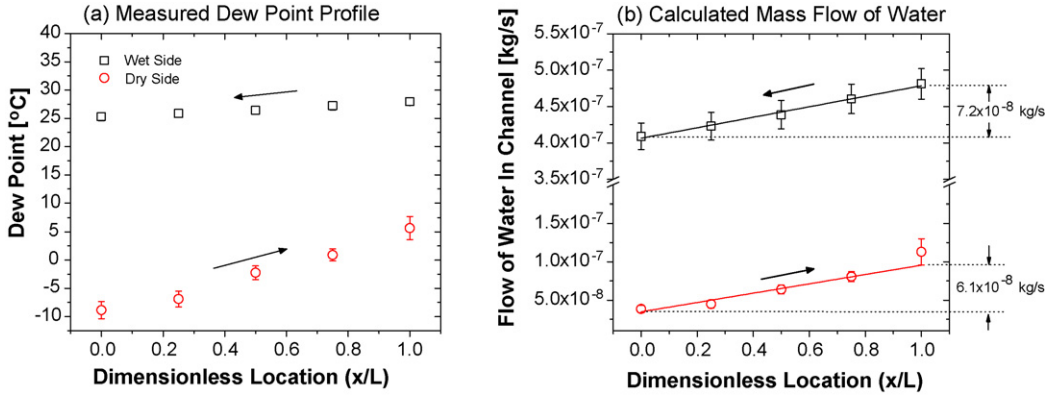

Fig. 13. Moisture profiles—Case 2 (isothermal, 30 °C).

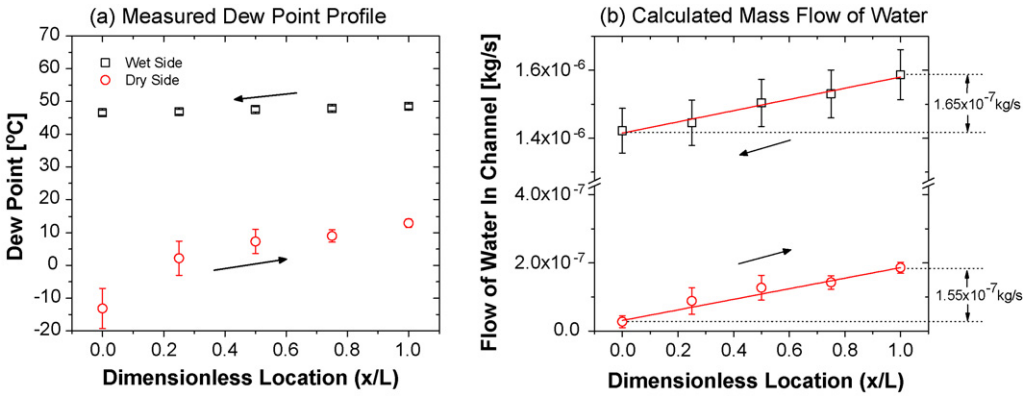

Fig. 14. Moisture profiles—Case 3 (isothermal, 50 °C).

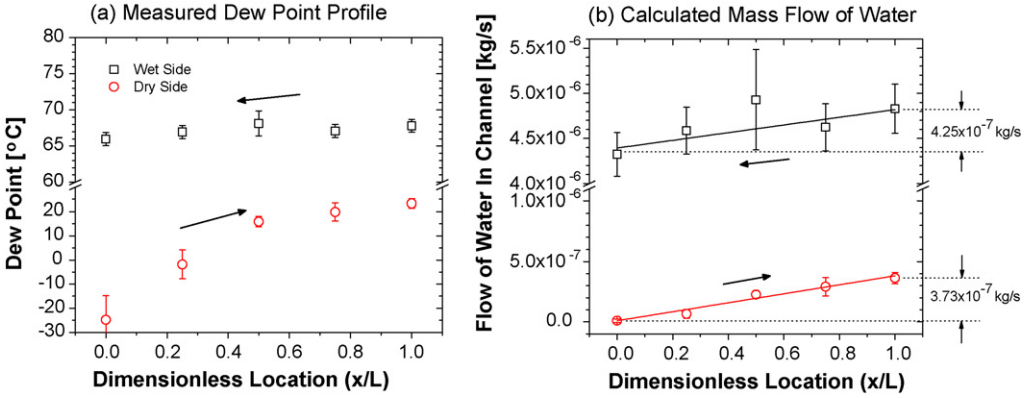

Fig. 15. Moisture profiles—Case 4 (isothermal, 70 °C).

70°. The reason for this is because the higher temperature dew points carry a lot more water into the system, but the humidifier is sized too small to transfer a significant portion of it to the dry side.

The estimated accuracy (based on sensor accuracy) and precision (standard deviation between replications) of these results are summarized in Table 3. At higher temperatures, even small error in measurement can result in large errors in the calculated values of average water flux and water recovery ratio.

4.3. Stream wise variation in moisture flux

The measured dew point profiles and calculated mass flow of water (Eq. (2) with $p^{sat}_{H_2O}$ replaced with the water vapour partial pressure p_{H_2O}) are shown in Figs. 12–15. For these figures, the arrows indicate direction of flow and the error bars shown are the manufacturer's stated accuracy limits or the standard deviation of the replications, whichever is higher.

In all cases, the mass flow rate of water in the channels (Figs. 12b, 13b, 14b, and 15b) appears to change linearly along the channel. Table 4 summarizes the fitted linear models. Although no phenomenological significance can be ascribed to the linear profile, it provides a useful empirical correlation for engineering design. A linear profile implies that the flux across the membrane is approximately constant along the length of the channel.

With the net change in water flow rate presented in the margins of Figs.12b–15b, it is possible to compare the amount of water lost from the wet side to the amount of water gained by the dry side. Although the difference was only statistically significant in Case 1, the amount of water 'lost' by the wet side is slightly higher than the water being 'gained' by the dry side stream. The possibility of a leak is unlikely; a more probable cause may be a result of measurement technique. As

Table 4
Calculated average water fluxes from Figs. 12b, 13b, 14b, 15b

	Calculated flux value ($\times 10^{-5}$ kg s^{-1} m^{-2})	Statistically different slopes[a]
Case 1		
Wet side	0.51	Yes
Dry side	0.26	
Case 2		
Wet side	3.60	No
Dry side	3.04	
Case 3		
Wet side	8.25	No
Dry side	7.76	
Case 4		
Wet side	21.3	No
Dry side	18.6	

[a] At a 0.05 significance level, determined by *t*-test.

mentioned in Section 2.3, the effect of concentration gradient across the channel may cause dry side measurements to be lower and wet side measurements to be higher than their true values.

5. Conclusions

An experimental investigation into the effect of operating conditions on a single channel gas-to-gas Nafion membrane humidifier has been carried out. A method for quantifying the heat loss rate to the surroundings per unit length was demonstrated by calculating an overall sensible heat transfer coefficient. For this particular geometry, a value of $0.149\,W\,K^{-1}\,m^{-1}$ was determined. This value is expected to change slightly with humid air, and change markedly in the presence of condensation on the walls.

The effect of flow rates on humidifier performance was studied by varying the dry side and wet side flow rates individually. In reporting results pertaining to moisture transfer, trends will vary depending on the metric used to indicate performance. The outlet dew point increases with lower dry side flow rates but was not significantly affected by wet side flow rates. The average water flux, however, did not follow the same trends since a higher outlet dew point or relative humidity seldom translates into better moisture transfer when comparing different flow rates. Certain flow rate combinations yielded optimum water flux across the membrane at each temperature, but these optimum flow rate combinations appear to be condition-dependent because no clear trend was uncovered with increasing temperature.

Finally, stream-wise dew point and mass flow of water profiles were presented. In the cases studied, moisture flux across the membrane did not vary significantly in the stream wise direction, and increased with higher operating temperatures.

Acknowledgement

The authors would like to acknowledge Natural Sciences and Engineering Research Council of Canada for financial assistance.

References

[1] M. Watanabe, H. Uchida, Y. Seki, M. Emori, P. Stonehart, J. Electrochem. Soc. 143 (12) (1996) 3847–3852.
[2] F.N. Buchi, S. Srinivasan, J. Electrochem. Soc. 144 (8) (1997) 2767–2772.
[3] J. Larminie, A. Dicks, Fuel Cell Systems Explained, second ed., John Wiley & Sons, West Sussex, England, 2003, pp. 75–90.
[4] W. Merida, PhD Dissertation, Mechanical Engineering, University of Victoria, Victoria, Canada, 2002, 204 pp.
[5] T.E. Springer, T.A. Zawodzinski, S. Gottesfeld, J. Electrochem. Soc. 138 (8) (1991) 2334–2342.
[6] Z.T.A. Jr., C. Derouin, S. Radzinski, R.J. Sherman, S.V.T.E. Springer, S. Gottesfeld, J. Electrochem. Soc. 140 (4) (1993) 1041–1047.
[7] J.T. Hinatsu, M. Mizuhata, H. Takenaka, J. Electrochem. Soc. 141 (6) (1994) 1493–1498.
[8] S. Ge, X. Li, B. Yi, I.M. Hsing, J. Electrochem. Soc. 152 (6) (2005) A1149–A1157.
[9] T. Okada, J. Electroanal. Chem. 465 (1) (1999) 1–17.
[10] D. Chen, H. Peng, J. Dynamic Syst. Measure Contr. 127 (3) (2005) 424–432.
[11] P. Berg, K. Promislow, J.S. Pierre, J. Stumper, B. Wetton, J. Electrochem. Soc. 151 (3) (2004) A341–A353.
[12] T.V. Nguyen, R.E. White, J. Electrochem. Soc. 140 (8) (1993) 2178–2186.
[13] L.Z. Zhang, Y. Jiang, J. Membr. Sci. 163 (1) (1999) 29–38.
[14] L.Z. Zhang, J.L. Niu, J. Heat Transfer 124 (5) (2002) 922–929.
[15] D.W. Johnson, C. Yavuzturk, J. Pruis, J. Membr. Sci. 227 (1) (2003) 159–171.
[16] R. Huizing, MASc. Dissertation, Chemical Engineering, University of Waterloo, Waterloo, Ontario, Canada, 2007, 73 pp.
[17] H.H. Voss, R.H. Barton, B.W. Wells, J.A. Ronne, H.A. Nigsch, US Patent 6,416,895 (2002).
[18] S. Park, E. Cho, I. Oh, Korean J. Chem. Eng. 22 (6) (2005) 877–881.
[19] F.M. White, Heat and Mass Transfer, second ed., Addison-Wesley Publishing Company, Inc., United States of America, 1988, p. 586.